PSSD EUROPE
Power Systems Design: Empowering Global Innovation

October 2012

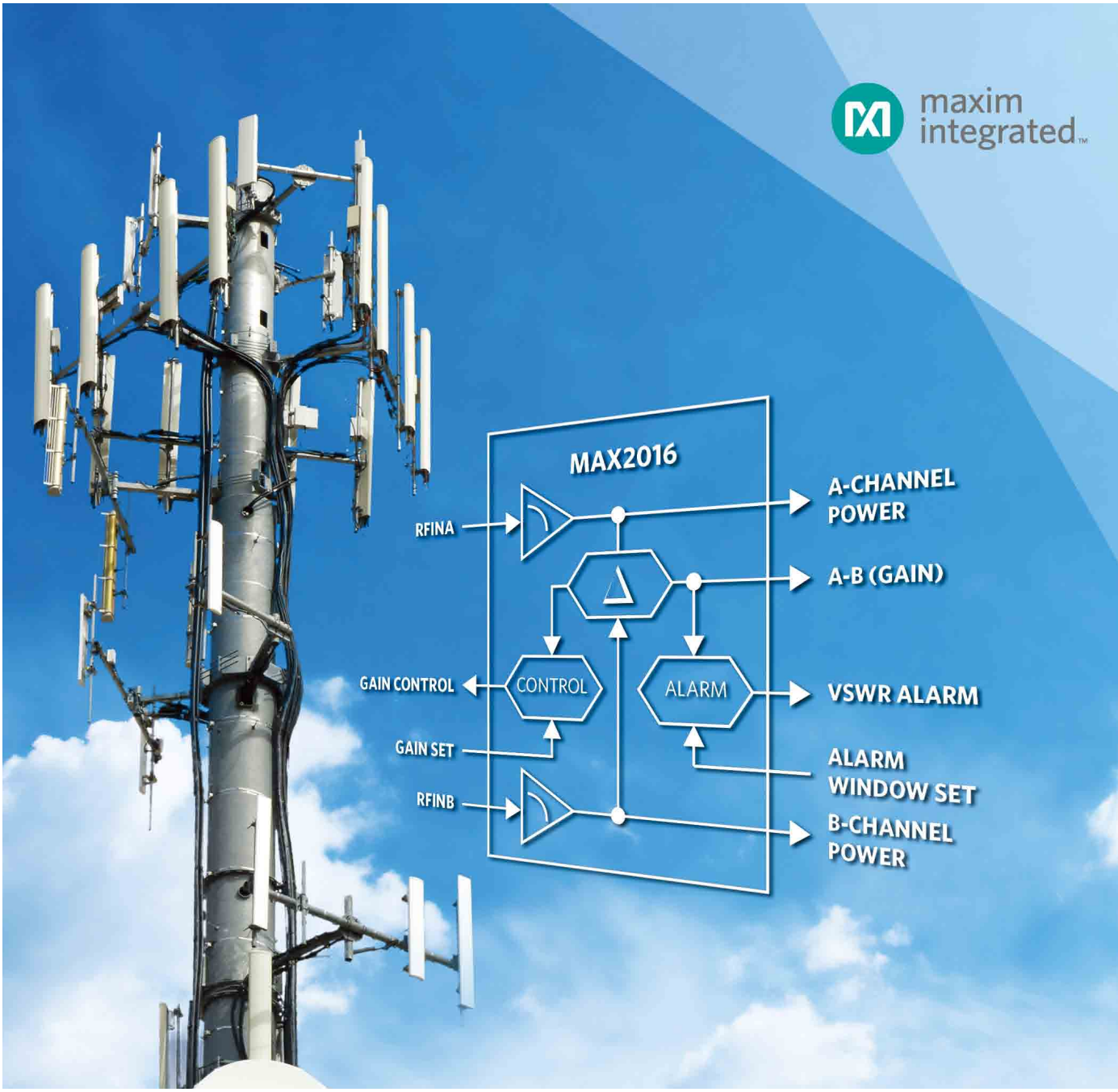

Special Report: Health, Medical, and Patient Mobility (PG34)

PSD EUROPE

Power Systems Design: Empowering Global Innovation

WWW.POWERSYSTEMSDESIGN.COM

Visit us online for exclusive content; Industry News, Products, Reviews, and full PSD archives and back issues

COVER STORY
Measure VSWR to quantify transmission-line imperfections (pg 15)

Highlighted Products News, Industry News and more web-only content, to:
www.powersystemsdesign.com

PSSD EUROPE

AGS Media Group
146 Charles Street
Annapolis, MD 21401 USATel:
+410.295.0177
Fax: +510.217.3608
www.powersystemsdesign.com

Editor-in-Chief
Joshua Israelsohn, Editor-in-Chief,
Power Systems Design
joshua@powersystemsdesign.com

Contributing Editors
Gail Purvis, European Editor,
Power Systems Design
Gail.Purvis@powersystemsdesign.com

Liu Hong, Editor-in-Chief, Power Systems Design China
powersdc@126.com

Ash Sharma, IMS Research
Ash.*sharma@imsresearch.com*

Dr. Ray Ridley, Ridley *Engineering*
RRidley@ridleyengineerng.com

David Morrison, How2Power
david@how2power.com

Publishing Director
Jim Graham
jim.graham@powersystemsdesign.com

Publisher
Julia Stocks
Julia.stocks@powersystemsdesign.com

Circulation Management
Kathryn Philips
kathryn.phillips@powersystemsdesign.com

Magazine Design
Louis C. Geiger
louis@agencyofrecord.com

Production Manager
Chris Corneal
chris.corneal@powersystemsdesign.com

Registration of copyright: January 2004
ISSN number: 1613-6365

Volume 9, Issue 8

Integrating electronics for detection and diagnosis

Chronic, non-communicable diseases (heart, cancer, respiratory, diabetes, kidney, and liver diseases) are, collectively, a challenge of epidemic proportions. At a global scale, they will cost an estimated $47 trillion by 2030. Europe currently has the highest number of deaths and disability due to these diseases according to the World Health Organisation. Yet according to the OECD (Organisation for Economic Co-operation and Development), on average only 3% of total health expenditure goes to public prevention with some 97% of health expenses spent on treatment.

Improved access to good quality air, water, food, and green space, and to sporting, recreational, and cultural facilities all contribute to reducing inequalities and creating sustainable communities. Improvement to housing conditions shows a number of positive effects on health, including lowering mortality rates while adequate heating systems improve asthma and reduce numbers of days off school in Europe.

Yet early detection and diagnosis are called for too. There is a need to develop new tools to detect chronic disease in at-risk populations. An interesting item to emerge recently is the Verisante Aura, an implementation of raman spectroscopy that evaluates skin lesions clinically suspicious for cancer. Approved for sale in Canada, Europe, and Australia, it is not yet accepted in Mexico, Brazil, or the USA. But Verisante is now working on a Core series of products with the same platform technology for the early detection of lung, colon, and cervix cancers.

Early detection is key to saving lives of melanoma patients and to saving on healthcare costs. A melanoma diagnosed and treated in the earliest stages results in a 99% survival rate and costs about $1,800 to treat. Detected and treated in later stages, survival rate drops to 15%; cost to treat soars to $170,000.

Small wonder that, operating in healthcare, Maxim Integrated, has taken as one of its catch lines “Analog integration” the “new prescription for medicine.” Diagnostics, monitoring, and therapy for healthcare it claims has simple math. Move point of care closer to patients, giving them the tools they need to care for themselves and that can reduce medical costs by 80%.

Tele-medicine is achievable, provided the broadband facilities are present. New tele-health technologies allow patients to receive long-term care at home, reducing costs from $5000/day for hospital stays to around $10/day. Ultrasound is portable. To take guesswork out of diagnosis and treatment and bring such benefits as cardiology to villages without electricity, let alone broadband, means systems designers must take heavy and expensive equipment and make it both smaller and more affordable.

As channel counts increase, in addition to space constraints, a new set of concerns arise as sensitive receive electronics are jostled by noisier digital electronics, and designers must search for ways to power all from fixed battery capacity. The answer it appears lies in integration.

Gail Purvis

Europe Editor
Power Systems Design
Gail.Purvis@powersystemsdesign.com

Imec, Holst Centre, and Panasonic develop brainwave headset

Imec, Holst Centre, and Panasonic have developed a new prototype wireless EEG (electroencephalogram) headset. The system combines ease-of-use with ultra-low power electronics. Continuous impedance monitoring and the use of active electrodes increases the quality of EEG signal recording compared to former system versions. Data is transmitted in real-time to a receiver located up to 10 m from the system. The realization of this prototype is a next step towards reliable high-quality wearable EEG monitoring systems.

The system integrates circuit-level components including Imec's active electrodes and EEG amplifier together with a microcontroller and a low-power radio. It is capable of continuously recording 8-channel EEG signals while concurrently recording ETI (electrode-tissue contact impedance). This simultaneous ETI recording enables continuous, remote assessment of electrode contact status during EEG recording.

The active electrodes reduce the susceptibility of the system to power-line interference and cable-motion artifacts, thus improving signal quality. The system can be configured at run-time to change the settings of the recordings such as the number of channels, or enabling/disabling the impedance recording. The autonomy of the system ranges from 22 hours (8 channels of EEG with ETI) to 70 hours (1 channel of EEG only).

The system has a high CMRR (> 92 dB), low noise (< 6 µV p-p, 0.5 - 100 Hz), DC offset tolerance of ±900 mV and is AC coupled with configurable cut-off frequency. Sensitivity and dynamic range are configurable through a programmable gain stage (default 1.5 mV pp and 366 nV, respectively).

The system (with dry electrodes and no skin preparation) is validated against a commercially available wired reference system (with wet electrodes and skin preparation), comparing the spectra between 1 and 30 Hz. The high correlation coefficients (ranging from 0.81 to 0.98 in four one-minute recordings with eyes open) indicate that both systems have similar performance.

The heart of the system is the low-power (750 µW) 8-channel EEG monitoring chipset. Each EEG channel consists of two active electrodes and a low-power analog signal processor. The EEG channels are designed to extract high-quality EEG signals under a large amount of common-mode interference. The active electrode chips have buffer functionality with high input impedance (1.4 GΩ at 10 Hz), enabling recordings from dry electrodes, and low output impedance reducing the power-line interference without using shielded wires.

The system is integrated into Imec's EEG headset with dry electrodes, which enables EEG recordings with minimal set-up time. The small size of the electronics system, measuring only 35 x 30 x 5 mm (excluding battery), allows easy integration in any other product.

See a video on the EEG headset at http://bit.ly/TJsyws

www.imec.be

www.holstcentre.com

Keeping up to date with medical-safety standards

By: Peter Blyth, Industry Director, Medical, XP Power

The 3rd edition of the 60601 medical-safety standard was first published by the IEC in 2005 (IEC60601-1:2005), was adopted by the EU (European Union) in 2006, and published as EN60601-1:2006. The AAMI (American Association for Medical Instrumentation) published the USA version, also in 2006, which appears as ANSI/AAMI ES60601-1:2006.

In Europe, as of 1 June 2012, the previous 2nd edition (EN60601-1/A2:1995) has been withdrawn and all products will need to be certified to the 3rd edition. The situation is rather different in the United States. The cessation date for 2nd edition (UL60601-1:2003 1st ed) is 30 June 2013 but, unlike the EU, the FDA only requires that new products brought to market after this date will need to be 3rd-edition certified.

One of the most significant changes that the 3rd edition introduces is that equipment manufacturers must now follow a formal risk management procedure that follows the ISO 14971 model. While the 2nd edition simply addressed basic safety issues to ensure freedom from any electrical, mechanical, radiation, and thermal hazards, it did not require devices to remain functional in that fail-safe was adequate, and compliance with test criteria relied upon a pass/fail result that did not take into account the essential performance of the device-under-test. Recognizing these limitations, the 3rd edition introduces specifications for *essential performance* that require that equipment will continue to function as its designers intended throughout the test process.

Within the electrical safety arena, the standard continues to require that equipment implement two MOPs (Means of Protection) such that if a failure occurs within one area, a second mechanism safeguards the operator and the patient against any electric shock hazard. The standard allows for three defensive approaches that manufacturers may use in various combinations: safety insulation, protective earth, and protection impedance. It is therefore essential to determine several key factors from the outset of the equipment design process, including its insulation class and its reliance on a protective-earth connection. Significantly, for power supplies, the 3rd edition distinguishes between protecting the equipment's operator and the patient within its MOOP (means of operator protection) and MOPP (means of patient protection) categories.

This distinction can result in quite different safety insulation and isolation requirements for circuits that operators and patients may contact. Specifically, anything that falls within the remit of operator protection only has to meet the clearance and creepage requirements that IEC/EN 60950 specifies for general-purpose information and technology equipment. In choosing a power supply with only MOOP, one would have to ensure other isolation schemes are in place between the output and the patient if the equipment is to contact the patient. No matter whether designers choose MOOP or MOPP, the standard still demands that equipment meets power-supply leakage-current requirements: 300 µA for the USA and 500 µA for the EU.

www.xppower.com

Power opportunities in the medical market

By: Jonathon Eykyn, Market Analyst, Power Management & Conversion, IMS Research, IHS

The opportunity for power-management companies supplying the medical market is both expanding and evolving. Shipments for high-end imaging equipment are growing as demand from China and other developing countries outstrips slowing growth in the developed world. Meanwhile, consumer-health products grow rapidly as the personal-health-care market develops.

This medical electronic-equipment market comprises mostly of imaging systems and consumer-health products, but includes surgical, orthopaedic and dental equipment, and prosthetics. According to new reports from IMS Research, the medical market for AC-DC and DC-DC merchant power supplies is estimated to be worth $460 million. The market for power semiconductors, including power ICs and discrete devices, is estimated at almost $450 million. The market is projected to grow strongly for both power supplies and power semiconductors with a five-year CAGR (compound annual growth rate) of 5 and 6%, respectively.

The medical market has historically been slow and steady for both power-supply and power-semiconductor manufacturers, dominated by high-cost, low-volume imaging machines such as ultrasound, MRI, and X-Ray. The high capital expenditure required for this equipment meant that the market was focused in developed regions such as Western Europe, North America, and Japan. Increasing affluence in developing regions has caused greater investment in healthcare, leading to higher demand for power-management products. This growth is balancing the slowdown in developed countries, particularly in Europe, where further healthcare spending cuts are expected due to their projected slower recovery from the recession.

One of the fastest growing markets is for consumer medical devices, driven by demand for telehealth gateways. These devices monitor vital signs from a patient in their own home and communicate the data to a central point. They require considerable data processing capability and data connectivity, including wireless. Integrated telehealth services communicate the data to health professionals for analysis. Shipments are projected to grow rapidly as they become more widely adopted over the next few years.

In contrast to the large, enclosed power supplies used in medical-imaging equipment, consumer-medical devices generally use external power adapters. This creates an entirely different opportunity that will be more cost driven. It is forecast that this sector will demand almost 90 million power supplies between now and 2016—a large opportunity for power-supply and power-semiconductor manufacturers.

Further semiconductor opportunities exist in battery-operated medical equipment. This is a wide market covering products from electric wheelchairs to pacemakers and portable diagnostic equipment. The availability of micro-power standard components suitable for hand-held, battery-powered equipment, developed as a response to the high volumes of consumer portable appliances, facilitates this change. This market is forecast to rise at between 6 and 7% through to 2016.

www.imsresearch.com

Z_{IN} measurements and filter interactions: Part 1

By: Dr. Ray Ridley, President, Ridley Engineering

In this article, Dr. Ridley continues the discussion of input impedance measurements, and shows the effect of properly locating all of the input filter components. Middlebrook's input filter stability criteria only apply to the system measured with the filter components in the correct location.

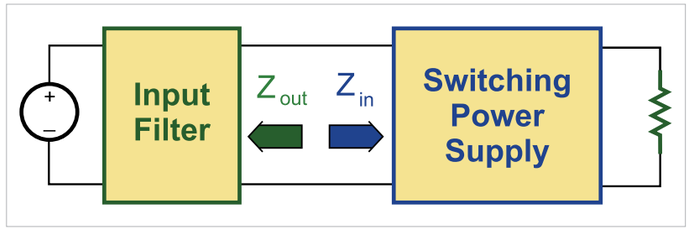

Figure 1: Power supply with input filter module

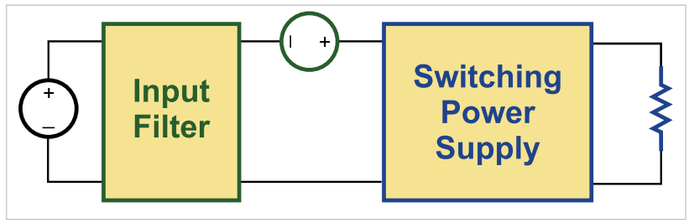

Figure 2: Voltage injection into the power rail for impedance interaction measurements

Input Impedance Measurements

As discussed in the last article, an input impedance measurement gives information about the characteristics of the power supply input terminals. The measurement is usually a requirement of the documentation package in the aerospace industry. The input impedance measurement is very useful for anyone that has to add components to the basic power supply design. This can include an input EMI filter, or another power supply that preconditions the input voltage rail.

Figure 1 shows a block diagram of a switching power supply connected to an input filter. Dr. Middlebrook, in his famous paper on input filter interactions, said that the if the input impedance of a converter, Zin, is always greater than the output impedance of the filter, Zout, then a stable power supply will remain stable when the filter is connected [2]. Measurements of both the filter output impedance, and the power supply input impedance are useful for predicting the stability of the resulting power system.

The impedances can be measured with the diagram shown in **Figure 2**. An ac voltage source is connected in series between the filter and the switching power supply. The input impedance is measured from the ratio of the input voltage of the supply and the current into the terminals. The output impedance of the filter can be measured with the same injection setup with the voltage probe at the output of the filter. The filter output impedance can also be measured with power removed from the circuit, as will be described in the next article. The practical implementation of the voltage injection and measurement is described in detail in [1].

The Middlebrook criteria require that the power supply block of Figure 2 contains only the

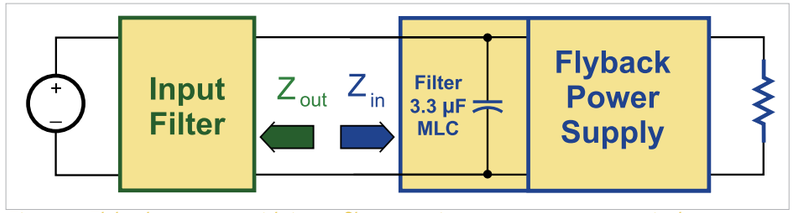

Figure 3: Flyback converter with input filter capacitor. In most cases, practical measurements require some input filter components to be included in the impedance measurement.

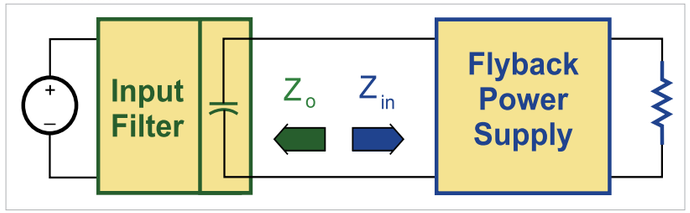

Figure 4: Proper characterization of the impedance interaction requires the input filter capacitor to be moved to the filter module.

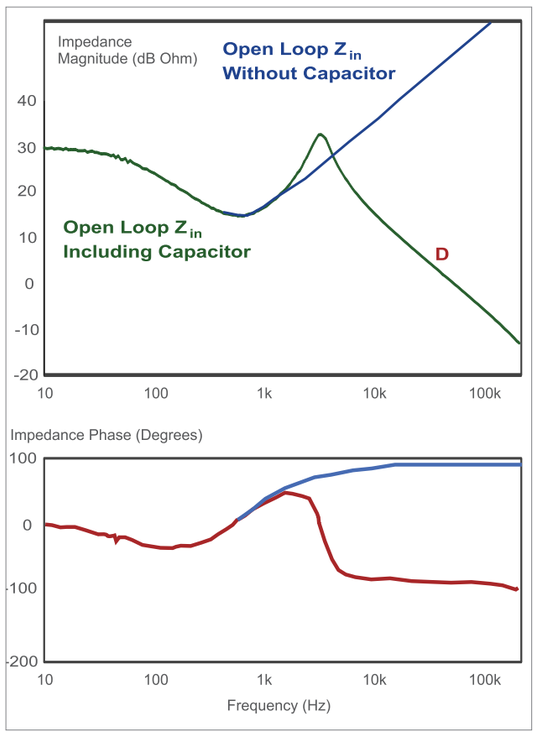

Figure 5: Open-loop input impedance measurements of a flyback converter with and without input capacitor.

switching cell, and none of the input filter components. However, it is usually a practical necessity that at least one filter component is included in the power supply block to filter high-frequency pulsating currents. Without this, measurements can be too noisy and the converter may not operate properly. Also, in many cases, the internal circuit nodes for measurement are inaccessible, and the power supply input impedance measurement will include several filter components.

Figure 3 shows a measurement setup where a small input bypass capacitor is included in the power stage measurements. As we will see, this has a significant impact on the input impedance measurements, greatly reducing the impedance at higher frequencies.

Figure 4 shows the proper location for application of the Middlebrook criteria. The filter capacitor is moved into the input filter block, and is not included in the power supply block.

Figure 5 shows the effect of the capacitor location on the open-loop input impedance measurements. The curve shown in green is the input impedance measured with the capacitor at the front of the power supply. The final impedance follows the asymptote D. Notice that the final value of the phase measurement is -90 degrees, corresponding to the capacitive impedance.

If the capacitor is moved to its proper place at the output of the filter block, the curve shown in blue results. Notice that the input impedance is much higher for this situation at higher

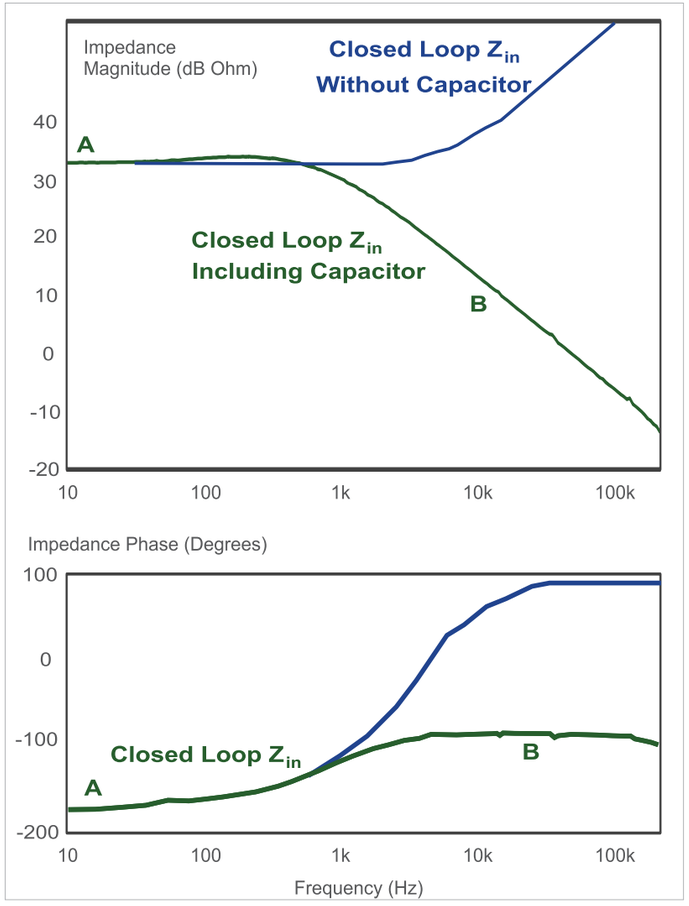

Figure 6: Closed-loop input impedance measurements of a flyback converter with and without input capacitor.

frequencies. The final asymptote is determined by the inductor of the power stage.

Figure 6 shows the input impedance of the same converter with the control loop closed. If the measurement is made without the input capacitor, the impedance is flat at low frequencies, with a negative value, and rises beyond the crossover frequency of the control loop. This is shown by the blue curve.

If the input capacitor is included in the measurement, the impedance drops substantially at higher frequencies.

For the power supply in this article, the input capacitor on the right of the measurement point is a small 3.3 µF multilayer ceramic. It is possible in this case to subtract the impedance of the capacitor from the measurements to predict the input impedance with the capacitor removed. In many real world supplies, it is not possible to modify the filter component connection or to get at the necessary circuit nodes. Large values of capacitor can be included in the measurements, and this makes proper application of the Middlebrook criteria very difficult.

Summary

This article discusses the significance of power supply input impedance with respect to the input filter interaction criteria. It is shown how small filter components included in the input filter measurements interfere with proper application of the Middlebrook criteria. In the next article, measurements of the input filter output impedance will be discussed to show how this can interact with the power supply.

References

1.Ridley Engineering Design Center, www.ridleyengineering.com/index.php/design-center.html, Article [59] Input Impedance Measurements.

2.“Power Supply Design. Volume 1: Control”, by Dr. Raymond B. Ridley. Full-color textbook available at http://www.ridleyengineering.com/index.php/books.html.

www.ridleyengineering.com

Measure VSWR to quantify transmission-line imperfections

Simple measurements provide insight into transmission efficiency

By: Wilson Tang, Member of Technical Staff, and Tom Au-Yeung, Director of Customer Applications, Maxim Integrated

Impedance mismatches in an RF transmission line causes power loss and reflected energy. The VSWR (voltage standing-wave ratio) is a way to measure transmission line imperfections.

In an RF electrical transmission system, the SWR (standing-wave ratio) is a measure of how efficiently RF power transmits from the signal-power source, through the transmission line, into the load. A common example is a power amplifier connected through a transmission line to an antenna.

The SWR is, thus, the ratio between transmitted and reflected waves. A high SWR indicates poor transmission-line efficiency and reflected energy, which can decrease transmission efficiency and damage the transmitter. Since the SWR commonly refers to the voltage ratio, RF engineers usually refer to it as the VSWR.

VSWR and system efficiency

In an ideal system, 100% of the energy transmits from the power stages to the load. This requires an exact match between the source impedance, that is, the characteristic impedance of the transmission line and all its connectors, and the load's impedance. The signal's AC voltage will be the same from end to end since it passes through without interference.

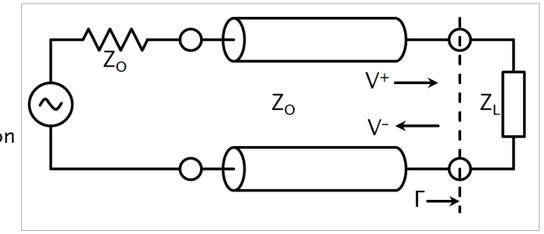

Figure 1: Transmission line circuit illustrating the impedance mismatch boundary between the transmission line and the load. Reflections occur at the boundary designated by Γ. The incident wave is V+ and the reflective wave is V-.

In real systems, however, mismatched impedances cause some of the power to reflect back toward the source, like an echo. Reflections cause constructive and destructive interference, leading to peaks and valleys in the voltage at various times and distances along the line. VSWR measures these voltage variances. It is the ratio of the highest voltage anywhere along the transmission line to the lowest voltage.

Since the voltage does not vary in an ideal system, its VSWR is 1.0 or, as commonly expressed as a ratio of 1:1. When reflections occur, the voltages vary and VSWR is higher, for example 1.2, or 1.2:1.

Reflected Energy

When a transmitted wave hits a boundary such as the one between the lossless transmission line and load, some energy will transmit to the load and some will be reflect back to the source (Figure 1). The reflection coefficient relates the incoming and reflected waves as:

(eq1)

$$\Gamma = \frac{V^-}{V^+}$$

where V— is the reflected wave and V+ is the incoming wave.

The VSWR relates to the magnitude of the voltage reflection coefficient, Γ, by:

(eq2)
$$VSWR = \frac{1+|\Gamma|}{1-|\Gamma|}$$

An SWR meter can directly measure VSWR . An RF test instrument such as a VNA (vector network analyzer) can measure the reflection coefficients of the input port, S_{11}, and the output port, S_{22}. S_{11} and S_{22} are equivalent to Γ at the input and output port, respectively. The VNAs with math modes can also directly calculate and display the resulting VSWR value.

You can calculate the return loss at the input and output ports from the reflection coefficient, S_{11}, or S_{22} as follows:

$$\text{ReturnLoss}_{IN} = 20\log_{10}\left(|S_{11}|\right)\ \text{dB}$$

$$\text{ReturnLoss}_{OUT} = 20\log_{10}\left(|S_{22}|\right)\ \text{dB}$$

Calculate the reflection coefficient from the transmission line's characteristic impedance and the load impedance as follows:

(eq3)
$$\Gamma = \frac{Z_L - Z_O}{Z_L + Z_O}$$

where Z_L is the load impedance and Z_O is the transmission line's characteristic impedance.

You can also express VSWR in terms of Z_L and Z_O. Substituting eq 3 into eq 2,

$$VSWR = \frac{1+\left|\frac{Z_L - Z_O}{Z_L + Z_O}\right|}{1-\left|\frac{Z_L - Z_O}{Z_L + Z_O}\right|}$$

$$= \frac{Z_L + Z_O + |Z_L - Z_O|}{Z_L + Z_O - |Z_L - Z_O|}.$$

For $Z_L \succ Z_O$,

$$|Z_L - Z_O| = Z_L - Z_O.$$

Therefore,

$$VSWR = \frac{Z_L + Z_O + Z_L - Z_O}{Z_L + Z_O - Z_L + Z_O}$$

$$= \frac{Z_L}{Z_O}.$$

For $Z_L \prec Z_O$,

$$|Z_L - Z_O| = Z_O - Z_L,$$

and

$$VSWR = \frac{Z_L + Z_O + Z_O - Z_L}{Z_L + Z_O - Z_O + Z_L}$$

$$= \frac{Z_O}{Z_L}.$$

As noted above, VSWR is a specification given in ratio form relative to 1, as an example 1.5:1. There are two special cases of VSWR, ∞:1 and 1:1. A ratio of infinity to one occurs when the load is an open circuit. A ratio of 1:1 occurs when the load matches perfectly to the transmission-line characteristic impedance.

The VSWR definition from the standing wave that arises on the transmission line itself is:

(eq4)
$$VSWR = \frac{V_{MAX}}{V_{MIN}}$$

where V_{MAX} is the maximum amplitude and V_{MIN} is the minimum amplitude of the standing wave. With two superimposed waves, the maximum occurs with constructive interference between the incoming and reflected waves. Thus:

(eq5)
$$V_{MAX} = V^+ + V^-$$

for maximum constructive interference. The minimum amplitude occurs with deconstructive interference, or:

(eq6)
$$V_{MIN} = V^+ - V^-$$

Substituting eq 5 and eq 6 into eq 4 yields

(eq7)
$$VSWR = \frac{|V_{MAX}|}{|V_{MIN}|}$$

$$= \frac{V^+ + V^-}{V^+ - V^-}.$$

Substitute eq 1 into eq 7, we obtain:

$$VSWR = \frac{V^+\left(1+|\Gamma|\right)}{V^+\left(1-|\Gamma|\right)}$$

$$= \frac{1+|\Gamma|}{1-|\Gamma|},$$

which matches eq 2, above.

VSWR Monitoring System

Modern RFICs simplify VSWR measurements. For example, the MAX2016 is a dual logarithmic detector/controller that, with a circulator and attenuator, can monitor the VSWR and return loss of an antenna. The MAX2016 outputs the difference between the two power detectors.

The MAX2016 in combination with a digital potentiometer, such as the MAX5402, and ADC, such as the MAX1116/MAX1117, forms a complete VSWR monitoring system (Figure 2). The digital potentiometer acts as a voltage divider by using the MAX2016's reference voltage output. The internal reference voltage can typically source 2 mA. This voltage sets the threshold voltage for the internal comparator (pin CSETL).

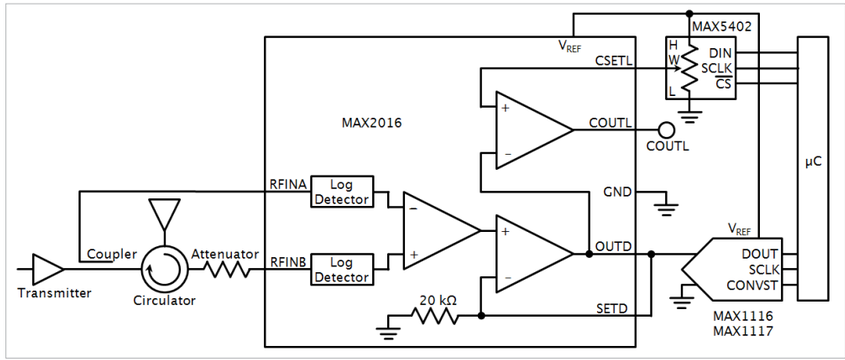

Figure 2: The VSWR monitoring system consists of an ADC for real-time measurements. The external digital potentiometer enables a configurable alarm signal at the comparator's output (COUTL).

The MAX2016 can generate an alarm when the output voltage crosses the threshold (pin COUTL). The MAX1116 ADC requires a 2.7 to 3.6 V supply, while the MAX1117 ADC requires 4.5 to 5.5 V. The ADC can also use an external reference voltage, provided by the MAX2016. The ADC paired with the microcontroller allows for constant monitoring of the antenna's VSWR.

www.maximintegrated.com

The 60-W TV

Cost-neutral adaptive backlight control improves energy efficiency

By: Paul Wilmarth, Director, Consumer Segment Marketing, ams

TVs in households are regular companions for many people around the world. It is common that people have the TV on in a living room while preparing a meal in the kitchen. In many cases, the TV is not being watched but only heard. With an average usage of four to five hours per day, every day, the TV is one of the biggest consumers of power in a household. Almost every household has a TV; some have as many as five large-format TVs.

The ubiquity of the TV in every home led the CEC (California Energy Commission) in 2009 to craft aggressive power-saving goals for companies selling TVs in that state. These were the nation's first energy-efficiency standards for televisions and they mandated that new TVs with 58-inch or smaller screens sold in California should consume 33% less electricity by 2011 and 49% less electricity by 2013.

While aggressive, the goals were achievable with available electronics technologies. The move from CCFL to LED backlighting and the incorporation of ambient-light sensors are rapidly enabling even more drastic power savings at leading TV manufacturers. Today over half of the TVs for sale are back lit by LEDs and most have analog or digital sensors on board to adjust the backlight in a way that maintains picture quality while saving power in low ambient-light conditions.

Just as the CEC had influenced technology design in California, the U.S. Environmental Protection Agency and the U.S. Department of Energy's ENERGY STAR program did the same at a national level. While consumers are familiar with the blue and white ENERGY STAR label, few know what it actually means and both manufacturers and retailers had been lax in this area.

Initial ENERGY STAR guidelines were not very affective, only measuring power usage at 0 Lux (no ambient light) and 300 Lux (room with sunlight). Taking only two measurements on the light power curve allowed manufacturers to easily earn an ENERGY STAR rating by having an unusably dim screen at 0 Lux and a full bright screen at 300 Lux. Manufacturers would adopt a simple photo diode technology, creating the appearance that they could pass these unsophisticated measurements. However, since that time, the standards have become increasingly stringent, with a new level of performance required about every 18 months. One of the first design changes that TV OEMs made in response to new ENERGY STAR guidelines was the incorporation of light sensors.

With the introduction of ENERGY STAR 6.0 in the Spring of 2013, the requirements become even more challenging. For example version 6.0 calls for a 42" TV to consume just 62.8 W, and the maximum power any TV can consume—regardless of screen size—is 85 W.

Measurement of power use is more thorough too. Version 6.0.requires measurement at four levels: 10, 100, 150, and 300 Lux. (Evidence suggests that more than 75% percent of people watch TV in a room with ambient light less than 50 Lux.)

Analog photodiodes respond to IR energy present in the ambient light. Digital methods eliminate IR energy from the ambient-light calculation resulting in more-accurate readings at low light levels. TV OEMs will need to adopt such technology to accurately assess the light environment, communicate the environment to the processor, and adjust the backlight for optimal power savings and viewing experience for the customer.

Figure 1: The local-dimming function saves 10 to 20% of power on edge-lit systems (left) and 20 to 30% of power on direct back-lit TVs (right).

Today, commercially available technology for sensor-driven LED Lighting allows 46-inch-class TVs to consume just 60 W. Achieving this low dissipation requires TV OEMs to adopt three technologies: Local dimming, high-accuracy LED drivers, and intelligent digital light sensors.

The TV Chip must support local dimming. This function looks at the video content and decides which LEDs it can dim to save power in the display. This scalar then uses the LED drivers to reduce light in those columns, for edge lighting, or sectors, in the case of direct lighting. This local-dimming function alone saves 10 to 20% of power on edge-lit systems and 20 to 30% of power on direct back-lit systems (Figure 1).

Additionally, when we combine a smart digital light sensor with local dimming we realize an additional 20 to 30% power savings. The digital ambient light sensor looks at the ambient light level in the room (remember 75% of people watch TV in a dimly lit room) and adjusts the backlight to a lower power level. The impact of this is threefold, the TV has improved contrast ratio, which is noticeable and pleasing to the eye; there is no blinding or discomfort to the consumer by the overdriven display and substantial power savings is realized. OEMs can realize this additional power savings outside the HDTV chip or incorporate it into the TV-system software for additional cost savings.

Note that one of the biggest power users in consumer electronics today is the flat panel TV. Current estimates attribute 3 to 4% of global residential electricity consumption to TVs—about 168 TWh, representing roughly 27 megatonnes of CO_2 emissions in 2010. By 2015, efficiencies such as those described here can result in annual electricity savings of approximately 3.2 TWh, the equivalent of 1.2 megatonnes of CO_2.

Power-saving initiatives are not just in the US but global. The EU has adopted an energy-class system where products are ranked by power consumption: A+++, A++, A+, A, B, C or D. Most TVs today rank as an A, B, or C. By adopting sensor-driven LED backlight with local dimming, European manufacturers will be able to achieve the higher *A* rankings. China is also promoting energy conservation in new TV designs. Manufacturers can meet the majority of the Chinese guidelines by switching to LED backlighting. Manufacturers that export, however, will need to adopt the sensor-driven approach to have products marketable in the US and EU.

There is no cost penalty to manufacturers or consumers to adopt these sensor-driven lighting technologies. They already buy components for driving LED backlighting; they already have sensors in the TV. It is simply a matter of connecting these devices in an intelligent way to optimize the design. A recent study in North America shows that when it comes to TVs, there are two items at the top of consumers' wish lists: A low power HDTV design and better picture quality. Adopting the 60-W-TV approach delivers on both of these desires and it does so without increasing the TV price in the least.

www.ams.com

Reliability of copper wire bonding for power devices

Copper wire bonds offer performance advantages over gold but demand changes to the wire-bonding process

By: Dr. Arthur Chiang, Director of Reliability Engineering, Vishay Siliconix

Though copper wire bonding developed nearly 30 years ago, it has only recently gained in popularity due to the rapid increase in the price of gold, which is now about 7,000 times that of copper (**reference 1**). It's well known that, compared to gold, copper has better electrical and thermal properties. Why, then, did it take such a global financial event for the technology to come out in force?

The primary concern lies in copper's chemical and mechanical properties. Chemically, copper easily oxidizes in air—witness the Statue of Liberty! Mechanically—though it has higher elongation and breaking load—copper is harder, which makes bonding to semiconductor devices more difficult and more prone to cracks under the bonds. This holds true for copper wire and FAB (free air ball), a term used by the semiconductor industry to describe the wire bond before it touches the semiconductor surface, which is usually coated with a thin layer of aluminum. Despite these shortcomings, however, copper does possess some superior properties, including better electrical and thermal conductivity. Better electrical conductivity means higher device performance or less material used. Better thermal conductivity translates into quicker heat dissipation and increased reliability of the device. Though this is counterintuitive, $R_{DS}(ON)$ measurements of power MOSFETs using both copper and gold wire bonds clearly show that using copper achieves a lower $R_{DS}(ON)$.

There are other important benefits of using copper bonding wires, but the key for their proliferation in semiconductor devices is still to overcome the difficulty created by the material's oxidation and hardness. To that end, the wire-bond industry has invested heavily and conducted a vast volume of study to optimize the design of the wire-bond mechanism and the process parameters to achieve wire bonds with good adhesion without peeling the substrate metallization or creating cracks in the semiconductor underneath. A few key innovations have developed: First, to overcome the oxidation problem, a flow system supplies a sufficient amount of a hydrogen-nitrogen mixture—*forming gas*—while FAB forms by the EFO (electronic flame-off) process, which uses a torch to melt the metal wire into FAB. A wire bond forms after this FAB touches the surface of the semiconductor device. In contrast, gold wire does not require a forming-gas flow system, and needs only a normal EFO box instead of the heavy-duty box required by copper.

Even with these advances in wire-bonding equipment, Vishay Siliconix engineers spent a few years working with equipment manufacturers to perfect wire bonding technologies. Many process-control measures are in place to ensure the quality and reliability of copper wire bonding (**Table 1**).

In developing the copper wire-bonding technology, Vishay Siliconix engineers have also discovered that innovative analytical techniques play a crucial role in building reliability into the new technology. For example, a major reliability concern in any wire-bond technology is the integrity of the device structure beneath the bonds. As a process-control tool, how much metallization remains under a bond—separating it from the device structure—is a key parameter.

			Cu	Au
Material & Tool	Wire	Storage	Inert gas pack	Normal
		Life	Work-life control	No work-life control
	Capillary	Life	Yes	Yes
Oxidation Prevention	Forming gas		Composition and flow rate	No
	EFO kit		Oxidation prevention EFO system	Open EFO system
	FAB making sequence		Before boding cycle starts	Before bonding cycle ends
Monitor	FAB		Spherical & shiney appearance	Spherical
	Function test		Ball shear / Wire pull / Copper etching method	Ball shear / Wire pull / Gold etching method
	Cross section		Flat interface profile & min top metal remaining limit	Flat interface profile

Table 1: Process-control measures

A good procedure for determining it requires three steps: First, polish the plastic mold compound from the top of the devices until the head of the bondwires appear. Next, use a FIB (focused-ion-beam) to mill through one of the bonds in a thin slice. Finally, measure the distance between the aluminum metal and FET structure. This technique precludes the use of any chemical, and thus preserves the state of the bondwire/top-metal interface for bonding study.

Using this technique, one can also study IMC (intermetallic compound) growth between the bondwire and the top metal. Compared to either bonding wire or aluminum top metallization, IMC is more brittle and carries higher electrical resistance. Therefore, slower IMC growth is beneficial to device performance and long-term reliability. Researchers have reported IMC growth under typical burn-in or temperature cycling conditions, but not for the most relevant condition: power cycling.

With a roughly equal initial aluminum thickness—4.13 µm for gold and 4 µm for copper—IMC is much thicker in gold wire-bonded parts at both the beginning and end of the conventional 15,000 cycles of power cycling. IMC grows to 11 µm in gold wire-bonded parts, but only 1 µm in copper.

Conversely, IMC to die top metal is less in gold wire-bonded parts in the beginning—1 µm for gold and 2.5 µm for copper—and ends with IMC directly in contact with the die top. For copper wire-bonded parts, IMC is still 2 µm above the die top even at the end of 15,000 cycles (**figure 1**).

Another way to look at the effect of IMC is to examine the wire pull strength after high- temperature storage (**figure 2**). The figure

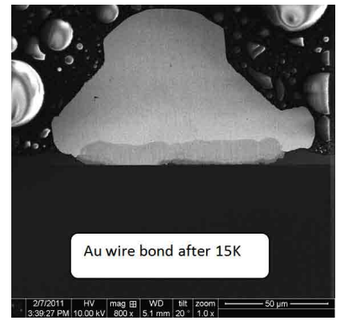

Figure 1a

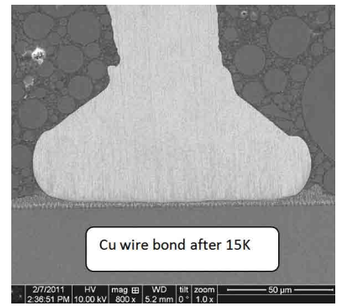

Figure 1b

Figure 1: After 15,000 cycles of power cycling, IMC grows to 11 µm in gold wire-bonded parts (A) but only 1 µm in copper (B).

compares the wire pull strength of copper and gold wire bonds over the course of a storage test. While copper bond strength stays relatively flat through the 6000-hour test span, gold wire bonds start to fail after 4,000 hours.

It should be clear by now that, though copper wire-bonding technology initially faced formidable challenges, advances in the design of wire-bonding equipment and the optimization of the bonding process have overcome those difficulties. So, now it is time to enjoy the benefits brought about by copper wire

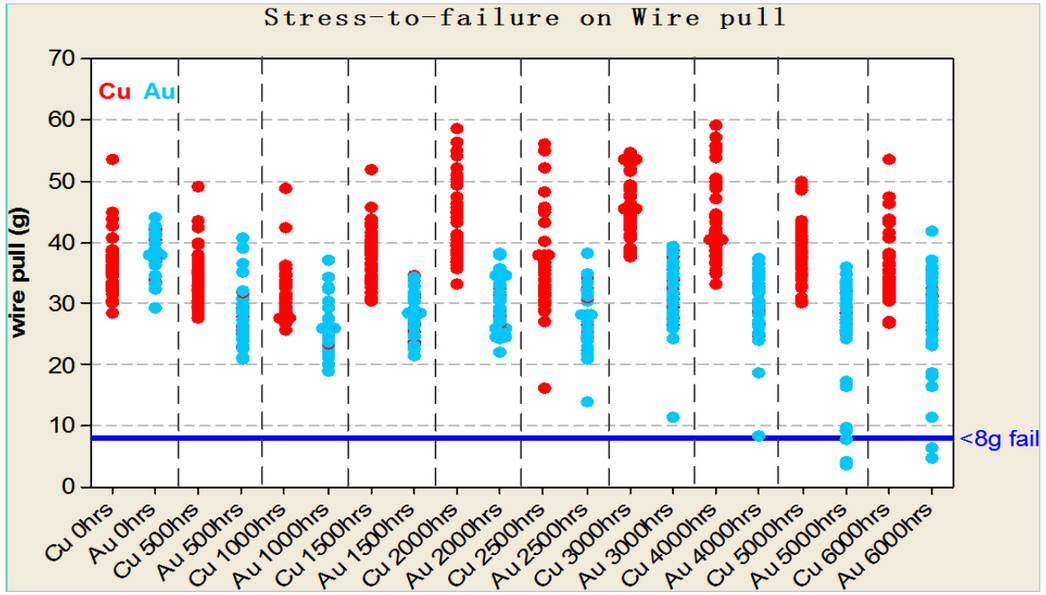

Figure 2: While copper-bond strength stays relatively flat through the 6000-hour test span, gold wire bonds start to fail after 4,000 hours.

	Copper Wire		Gold Wire	
Package	**Sample Size**	**Bond Failure [ppm]**	**Sample Size**	**Bond Failure [ppm]**
TSOP6	3525	0	3820	0
SOIC8	6060	0	3585	0
PPAK1212	2720	0	3450	0
PPAKSO8	3010	0	1150	0
Process Family				
A	5412	0	9020	0
B	4510	0	5084	0
C	3690	0	2952	0
D	7790	0	5330	0

Table 2: Reliability data for copper- and gold-wire-bonded parts

and its superior mechanical, electrical, and thermal properties.

The slower IMC growth in copper wire bonds can also extend the usable life of copper-wire-bonded parts. In order to prove their reliability, Vishay Siliconix tested copper-wire-bonded parts at twice the duration required by the standard industry specification. Reliability testing included temperature cycling (– 65 to +150 °C), HTGB (high-temperature gate bias), HTRB (high-temperature reverse bias), HAST (highly accelerated stress test), and PPOT (pressure pot).

Part of this study compared the performance of copper- and gold-wire-bonded parts in four package types and in four silicon process technologies used in mass production (**table 2**). The results show that, as far as we can measure, copper-wire-bonded parts are just as reliable as gold-wire-bonded parts.

www.siliconix.com

References:

1. J. Kurtz et al., *Copper wire ball bonding*,Proc. IEEE Electronics Components Conf., May 1984.
2. H. Wu, A. Chiang, D. Le, and W. Pratchayakun, *Failure analysis on power MOSFET devices with copper wire bonds*, Proc. 37th International Symposium for Testing and Failure Analysis, Nov. 2011.

Reducing standby power consumption for LED Lighting

A small circuit modification allows synchronized burst-mode operation of the PFC and DC-DC stages in a two-stage SMPS

By: WonSeok Kang, Senior Application Engineer and Youngbae Park, Application & System Engineering, Power Conversion, Fairchild Semiconductor

LEDs provide high-efficiency, environment-friendly characteristics, and a long life compared to conventional lighting sources. Therefore, they are becoming a primary light-source choice to reduce energy consumption in both internal and external lighting.

A switching power supply designed to power-up LED lamps should also exhibit high efficiency to match the energy-saving nature of the LED lamp. In addition to high power-conversion efficiency during normal operation, the switching power supply's standby power consumption has also become a popular focus for the LED industry.

It is expected that standby power consumption will be regulated to less than 1 W or even 300 mW in the near future. LED lighting applications, however, have not adopted an auxiliary power stage dedicated to the standby power supply primarily because the lighting applications do not have a standby mode during operation. However, the switching power supplies powering LED lamps still connect to the grid and draw power even with no lamps lit or under broken-lamp conditions. This is a primary source of concern for standby-power levels in lighting applications.

Lighting systems with poor standby power consumption in, for example, empty office buildings are not environmentally sound. Introducing a simple auxiliary circuit can reduce standby power consumption. This simple circuit enables burst-operation of the PFC (power factor correction) stage. A 120-W-rated two-stage switching power supply demonstrates the concept and achieves less than 1-W of standby power consumption over a wide input range.

Two-stage Configuration

Switching power supplies for LED street lighting typically use a two-stage configuration because of their power rating and need to improve power factor. The power supply comprises a PFC block for the first stage and a downstream DC-DC converter for the second stage.

At the medium power range—around 100 W—CRM (critical conduction mode) is an appropriate control scheme for the PFC stage. For the downstream DC-DC converter, a quasi-resonant flyback topology is popular at that power rating. Power controllers, such as the FAN6300 PWM (pulse-width modulation) controller, have an internal valley-voltage detector that ensures the power system operates in quasi-resonant mode under a wide range of line voltages, and reduce switching losses to minimize the switching voltage on the drain of the power MOSFET.

To minimize standby power consumption and improve light-load efficiency, a proprietary green-mode function provides off-time modulation to decrease switching frequency and performs extended valley-voltage switching to keep the MOSFET drain-source voltage at turn-off to a minimum level. With this feature, the second DC-DC stage enters burst-operation at no-load and can achieve very good standby power consumption.

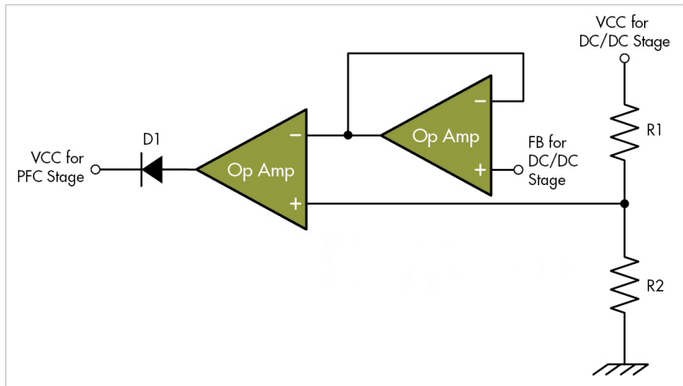

Figure 1: A simple control circuit implements PFC stage burst-mode operation.

Most existing PFC controllers do not have the burst-operation feature, mainly because the PFC-stage design usually targets consumer or display applications and the auxiliary power stage is separate in those cases that supply voltage to PFC and DC-DC stages. In LED lighting applications, which usually do not implement an auxiliary power stage, the PFC stage should be turned off or a standby-power-consumption rating less than 1 W is not possible.

PFC-stage burst operation

A major reason for shutting down the PFC stage is that most PFC controllers do not have a burst-operation feature. If a PFC controller does not support burst-operation, the PFC stage will operate constantly and draw power, even under no-load conditions. Therefore, shutting down the PFC stage is the only practical way for two-stage switching power-supply designs with existing PFC controllers to meet standby power consumption regulations. However, huge inrush currents conduct when the PFC stage restarts and cause increased voltage or current stresses on the MOSFET power switches.

This restart event may also result in flickering during constant-current operation of LED lamps. A new approach is required to meet the regulations for standby power consumption without these problems. A possible way to eliminate these side effects associated with a complete shutdown of the PFC stage is to implement PFC stage burst-mode operation.

A simple supplementary circuit synchronizes PFC operation with the quasi-resonant flyback DC-DC converter because the PFC stage can also enter burst-mode when the DC-DC converter starts burst-operation. The PFC stage quits burst operation as soon as the second-stage flyback converter ends operation in burst-mode.

Feedback from the quasi-resonant flyback DC-DC converter controls the bias supply for the PFC stage (**Figure 1**). When the feedback voltage from the flyback converter drops during no-load conditions, the supply voltage for the PFC stage is cut and the PFC controller stops operation.

The PFC stage starts burst-operation as soon as the second stage flyback converter enters burst-operation and stops burst-operation to synchronize with the flyback converter. By implementing burst-mode operation for the PFC stage, it is possible to eliminate large inrush currents that cause potential problems while dramatically reducing standby power consumption.

In order to evaluate the burst operation of the PFC stage, a 120-W (48-V, 2.5-A) rated LEB-016 demo board for LED street lighting is equipped with a FAN7930B CRM PFC controller, FAN6300A quasi-resonant flyback controller with burst-mode operation, and the PFC control circuit in figure 1. The PFC burst-mode implementation keeps the PFC and DC-DC stages synchronized (**Figure 2**).

Standby power consumption measurements at various line input voltages are shown in **Table 1**. Measurements at various input

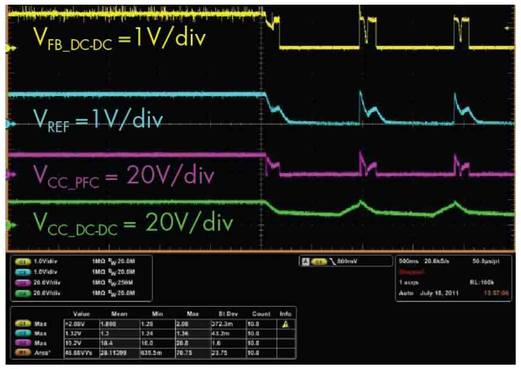

Figure 2a

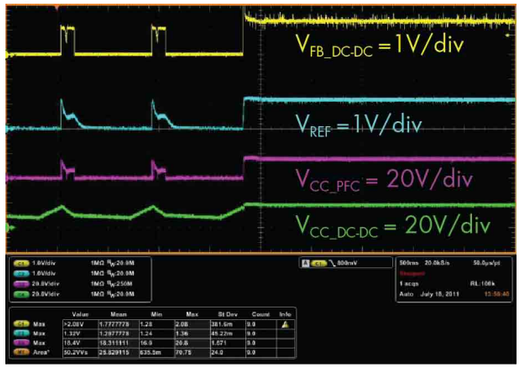

Figure 2b

Figure 2: When transitioning from full-load to no-load, both the PFC and DC-DC stages enter burst-mode operation (A). Both circuits exit burst mode when load current transitions again from no-load to full-load (B).

No Load Input Voltage [V AC]	PFC On [mW Avg]	PFC Off [mW Avg]	Reduction
100	500	60	88%
150	800	110	86%
200	1000	200	80%
230	1600	300	81%

Table 1: Standby power consumption

line voltages confirm that a more than 80% reduction in standby power consumption is attainable over a wide input range. Further, the maximum standby power consumption is 300 mW for high-line input.

www.fairchildsemi.com

Optimize data rates in isolated SPI buses

Isolating SPI clock, control, and data lines aids link robustness but requires timing and data-rate analysis.

By: He Junhua, Senior Technical Marketing Engineer, Avago Technologies

The simple SPI (Serial Peripheral Interface) bus is a popular serial interface commonly employed in automotive, industrial-control, and communications applications. To provide isolation and minimize the effect of ground loops, optocouplers are de-facto standard in these systems. They ensure data integrity and provide electrical safety in noisy and hazardous environments. However, adding optocouplers to the serial-data channel affects the data throughput. The SPI protocol bit timing depends on the data bit rate and optocoupler propagation-delay time.

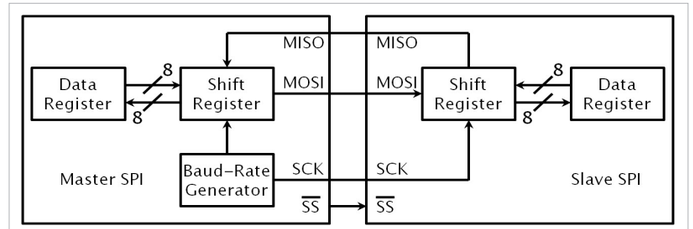

Figure 1: The 8-bit data registers in the SPI Master and Slave devices are linked by the MISO and MOSI signals to form a 16-bit control register.

SPI operation

The SPI bus provides a four-wire synchronous serial communication interface, often between an MCU and peripheral devices. The four wires are MISO (Master Input / Slave Output), MOSI (Master Output / Slave Input), SCK (Serial Clock), and $\overline{SS}$ (Slave Select or Chip Select). The main control element of an SPI subsystem is the SPI Data Register. There are two 8-bit data registers: one in the master and one in the slave. Together they form a 16-bit register linked by MISO and MOSI pins (**Figure 1**).

Only a master SPI module can initiate data transmission. A transmission begins by the host processor writing to the master data register. If the shift register is empty, the byte immediately transfers to the shift register and then shifts out on the MOSI pin under the serial clock's control.

Only the master SPI module generates the serial clock signal and synchronizes data communication with slave devices. A master SPI module usually configures the $\overline{SS}$ pin as a Slave Select output. Before data transmission occurs, the $\overline{SS}$ pin must assert low and remain low until the transmission is complete. Allowing $\overline{SS}$ to go high forces the SPI port into its idle state.

There are two types of SPI connections that include one master and multiple slaves: daisy-chain cascaded slave devices and parallel-linked slave devices. The slave device could also work with several masters via the multi-master protocol. Here, we focus only on the single master/slave connection because the timing sequence for multiple slave devices is similar to the timing for a single-slave connection.

Sometimes the SPI port communicates using only three wires. This is possible when a peripheral device is in a fixed configuration and only sends out data, eliminating the need for an

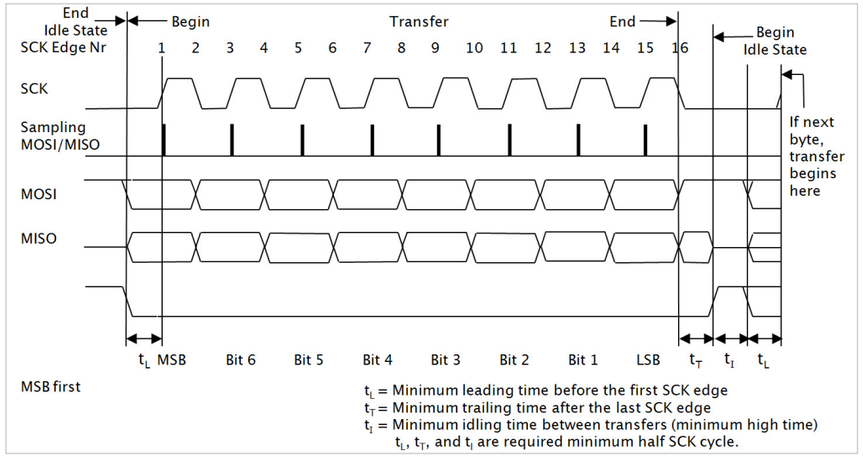

Figure 2: Data from the master SPI port is shifted into the slave device SPI port on the leading edge of the serial clock signal while data from the slave device's SPI port is simultaneously shifted into the master's SPI port as shown on the MOSI and MISO pins.

input signal. Similarly, or if the peripheral only inputs data then the bus can operate without the output signal.

The SPI timing chart illustrates the control settings for the SPI port (**Figure 2**): Clock active-high (CPOL=0), data sampling occurs at the clock's odd edges (CPHA=0), data transfers MSB first (LSBFE=0). A write or read to the master's data register initializes the data-transmission operation. In typical SPI data transmissions, the first clock edge issues a half cycle after $\overline{SS}$ goes low. The first edge on the SCK wire clocks the first data bit of the master shift register into the slave via MOSI and at the same time, the first data bit from the slave clocks into the master via MISO.

When the subsequent second edge on the SCK wire occurs, the previously latched data shifts into the shift register's MSB (most-significant bit). The same operation repeats through to the 16th edge of SCK at which point all eight data bits from the master have shifted into the slave and all eight data bits from the slave have shifted into the master. After the last bit shifts in, data are transferred into the parallel SPI data register from the shift register.

From the last clock edge, there is a minimum of a half clock cycle trailing time, tT, before the clock level goes high and SPI begins next idle state. The $\overline{SS}$ wire retains the high state for a minimum half clock cycle idling time, tI, before clock level goes low again.

TimingBefore inserting optocouplers into the SPI interface, let's analyze the relationship between the optocoupler's propagation-delay time and the signal data rate as it passes through the optocouplers. An optocoupler's maximum high-to-low and low-to-high propagation delay, (tPHL and tPLH), will indicate the device's maximum data transmission rate (**Figure 3**). The maximum propagation delay tP(MAX) is

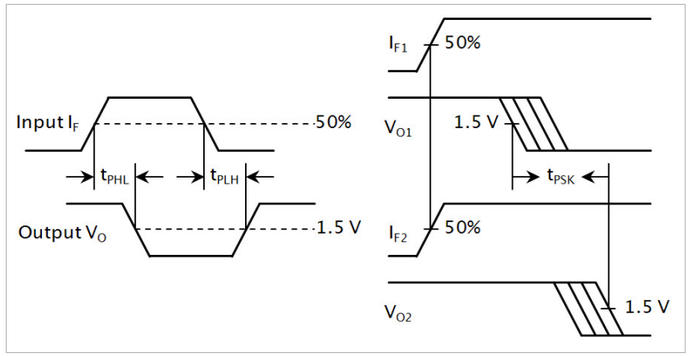

Figure 3: Optocoupler propagation-delay skew is the difference between the minimum and maximum propagation delays of tPLH and tPHL.

the greater of tPHL or tPLH. An optocoupler transmitting NRZ (non-return-to-zero) data requires that the data bit period, τ, is at least greater than tP(MAX):

$$\tau \geq t_{P(MAX)}$$

So, the maximum data rate is:

$$DR_{NRZ(MAX)} = \frac{1}{\tau} \leq \frac{1}{t_{P(MAX)}}$$

For a clock signal that employs RZ (return-to-zero) coded data, a clock cycle includes both the high and low period: τ = tHIGH + tLOW. For an optocoupler to transmit a 50% duty cycle clock signal requires that half a clock cycle be greater than tP(MAX):

$$\tau \geq 2t_{P(MAX}$$

Then the maximum clock frequency is:

$$f_{RZ(MAX)} = \frac{1}{\tau} \leq \frac{1}{2t_{P(MAX)}}$$

When data transmits synchronously over parallel signal lines, the optocoupler's propagation delay skew, tPSK, is an important factor that may determine the maximum parallel data transmission rate. If the parallel data transmits through two individual optocouplers or one multi-channel optocoupler, differences in the propagation delays between channels will cause the data to arrive at the optocouplers' outputs at different times—the skew. If this difference in propagation delay is sufficiently large, it will limit the maximum rate at which parallel data can transmit through the optocouplers.

Propagation-delay skew is the difference between the minimum and maximum propagation delays of tPLH and tPHL for any group of optocoupler channels operating under the same conditions of drive current, supply voltage, output load, and operating temperature (**Figure 3**). The optocouplers' tPSK will result in uncertainty in both data and signal lines. In general, the absolute minimum pulse width that can pass through parallel optocouplers is twice tPSK:

$$T_{PW} \geq 2t_{PSK}$$

The maximum data rate is, then:

$$DR = \frac{1}{T_{PW}} \leq \frac{1}{2t_{PSK}}$$

A conservative design should use a slightly longer pulse width to ensure that any additional uncertainties elsewhere in the circuit do not cause problems.

Continues at http://bit.ly/SWMTbr with timing and data-rate analysis for a sample isolated SPI implementation.

Editor's note: A complete presentation of this article is available online at http://bit.ly/SWMTbr

www.avagotech.com

Designing with digital power for optimum system performance

High efficiency and auto compensation benefit applications with large dynamic load currents

By: Ramesh Balasubramaniam, Marketing Director, and Håkan Karlsson, Field Application Engineer, International Rectifier

Digital power has emerged to satisfy the need for power supplies capable of handling the complex and rapidly changing power demands of high-performance computing subsystems. These include equipment for applications such as internet or telecom switches, enterprise servers, data-centre equipment, and graphics workstations.

A typical application using digital power consists of one or more high-performance processors, FPGAs or ASICs, along with DDR memory and multiple I/O ports. The key processing and memory components in the subsystem may require multiple VRs (voltage regulators), some of which may need specialised digital interfaces such as VID (Voltage Identifier), I²C, or Power Management Bus (Digital Power Technology).

When designing the power supply, the effects of factors such as interactions and interdependencies between chips, sequencing issues, and power management must also be taken into account. In addition, the latest nanometre-scale IC process nodes demand lower operating voltages and greater precision in terms of accuracy, temperature stability, and transient response.

Faced with such challenges, established analogue control techniques can struggle to maintain continuous, tightly regulated power as load currents change continuously and rapidly over a wide range. Designers working with conventional power supplies must also contend with time to market pressures that typically demand greater focus on the system design rather than the power supply. Limitations on PCB real estate also compromise designers' ability to optimise the power supply layout for minimum susceptibility to noise.

Digital power controllers can overcome these challenges and enable a smaller implementation than conventional controllers can. They do so while offering powerful capabilities such as dynamic adjustment, adaptive response, and auto compensation to help maintain stable power across the spectrum of operating conditions. In addition, the online design tools for configuring this new generation of devices allow designers to collect real-time performance and diagnostic information from the controller on the customer's board.

Design Approaches

Engineers may design traditional analogue regulators using a spreadsheet, engineering calculation software such as Mathcad, or even paper and pencil. Typical design support for digital power controllers, on the other hand, integrates all tools within a single GUI. This significantly speeds up the design cycle and can improve the quality of the design, for example by plotting frequency response to aid stability analysis and allowing quick and accurate comparison of multiple simulations for easy optimisation.

The GUI is not only used for setting the parameters and designing the application, but can also be used to monitor the controller's status in real-time when it is operating on the customer's board. Input voltages and currents,

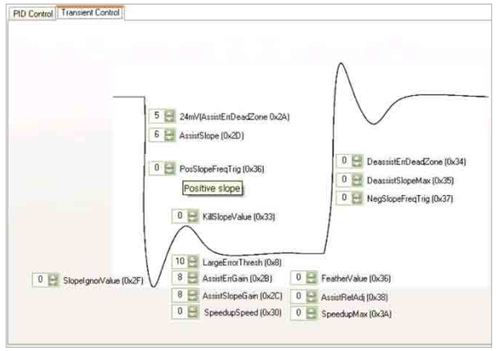

Figure 1: Optimising transient response parameters via a digital-power GUI.

output voltages and currents, and temperature all report dynamically, including individual phase currents. Fault status is also available, making identification and debug much faster.

With demand for extra channels and greater functionality within established form factors, designers effectively have less PCB real estate available for placing power components. It is increasingly difficult to achieve an optimal layout using traditional power topologies. Digital power, on the other hand, requires fewer components, and layout is less critical since the design is inherently more noise tolerant.

Designers can also gain the advantages of reduced BOM (Bill of Material) costs for external components, and can change design parameters by updating software rather than having to change a component on the board. The update executes via a connection such as I2C or Digital Power Technology, which can be used to monitor the controller's status. Often, inventory data such as model number, revision number, and manufacturer identification is available for read back.

Transient Response

Digital power delivers critical performance advantages by allowing the use of non-linear control algorithms in addition to the proven linear control techniques used in analogue power regulators. Non-linear control can allow optimisation of many parameters affecting different parts of the transient response (**figure 1**).

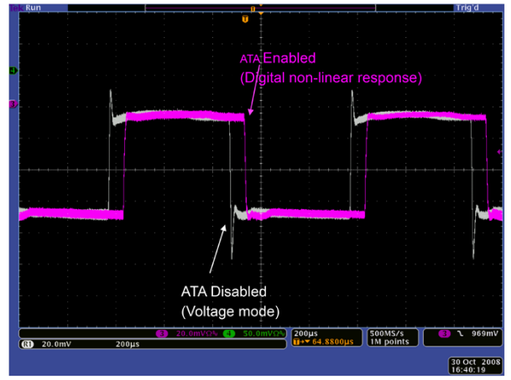

Figure 2: Non-linear control eliminates voltage overshoot and undershoot at abrupt load transients.

The designer may choose to use standard linear voltage-mode control during steady-state conditions and small transients, and apply a non-linear ATA (adaptive transient algorithm) for the duration of any large transient events.

The ATA is a non-linear closed-loop technique that uses the magnitude and slope of the monitored error signal to predict the current step and control pulse width and phase relationships accordingly. The power supply will typically operate in this mode for less than 10 µs and only during large transients. The designer can control the ATA through the GUI used for device configuration and monitoring. The designer can also optimise different parts of the response easily using graphical tools.

In **figure 2**, the grey waveform shows a digital power controller using only linear voltage-mode control. Overshoot and undershoot spikes are easily visible as the load steps on and off. The pink waveform shows how non-linear control effectively eliminates the undershoot and overshoot spikes under the same load-stepping conditions.

Optimising Efficiency

Digital power control enables designers to improve efficiency throughout the load range, from energy-saving standby modes to full power. It accomplishes this in part by using dynamic phase

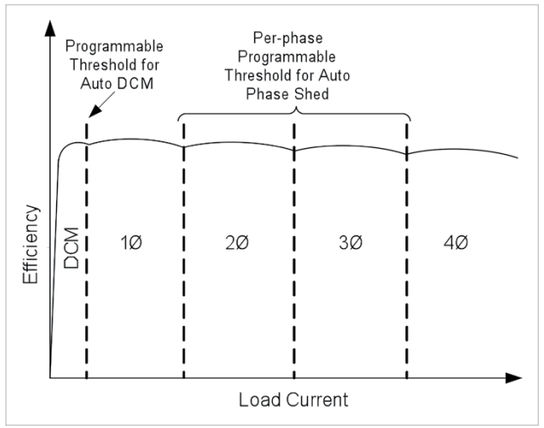

Figure 3: Dynamic phase control with preset load thresholds.

control with digitally scaled compensation to add or shed phases to satisfy varying system demand.

Analogue multi-phase voltage regulators typically allow two efficiency modes: with all phases turned on efficiency is good at maximum current, while single-phase operation is used to optimise efficiency at minimum current. Efficiency is less than optimal, however, in medium-current ranges. A digital controller is able to support preset phase-add and phase-drop points to ensure the optimum number of phases is active at a given output current level. In a 4-phase regulator, for example, drop points can be programmed to allow 1-, 2- ,3-, or 4-phase operation depending on load current (**figure 3**).

The key challenge in implementing dynamic phase control lies in adding phases. Whereas the controller can drop phases relatively easily and rapid response is generally not critical, phases must add quickly in response to a sudden increase in the load. A good digital power controller must add phases extremely quickly—in the nanosecond range—and must add the phases in the right sequence and timing to ensure that the output voltage does not undershoot below specification. Phases add based on the slope or magnitude of the error signal, which enables near-instantaneous response.

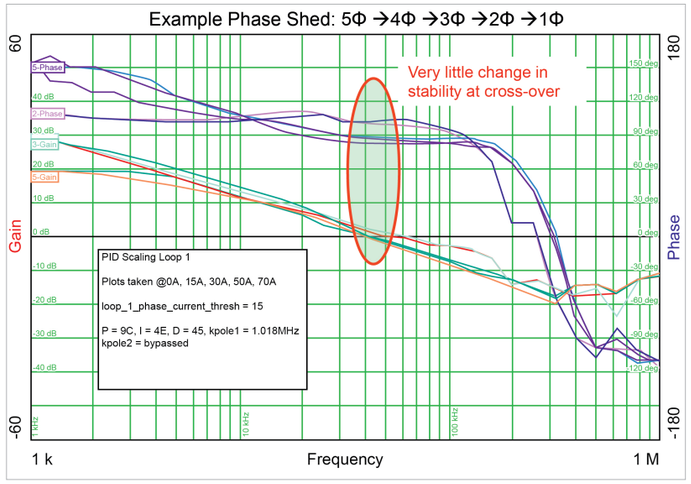

Figure 4: Phase shedding with minimal impact on power supply stability.

It is important to remember that a load oscillation could cause the controller to continuously add and drop phases. Under a load oscillation, it is better to keep more phases running to minimise disturbance at the output. Controllers can achieve this using a phase-drop filter with a preset limit such as 1.25 kHz and several Amperes of hysteresis to prevent spurious phase dropping during fast transients and to guard against phase *bouncing*.

It is also important to remember that adding or subtracting phases changes the operating conditions and, hence, the stability of the control loop. A digital controller can calculate and store all the different compensation parameters for each operating condition and apply them appropriately to ensure stability of operation. **Figure 4** shows how a five-phase controller essentially operates at the same stability point (cross over frequency and phase margin) irrespective of the number of phases running.

www.irf.com

Special Report: Health, Medical, and Patient Mobility

PSD EUROPE

Power Systems Design: Empowering Global Innovation

Inside:

Power management of an artificial hand

Balancing mass, function, and energy

By: Dr Paul H Chappell, Faculty of Physical and Applied Sciences, University of Southampton

For an upper extremity amputee, mass is a main factor when choosing an artificial hand. A hand should be lightweight so that high pressure points do not develop inside the plastic socket that attaches a hand to a person's residual limb. Also, the muscles of the arm and shoulder will have to work harder if a hand is too heavy and a high mass will cause people to reject the technology. A target hand mass is about 350 g.

Similarly the power source should be small and have low mass although the source can be attached proximally in a convenient place such as in the socket. In recent years, the advances in battery technology for communications applications have solved the battery problem for the prosthetic hand. As a minimum requirement, one battery pack will be in use with a fully charged spare and another one as a back-up. The typical voltage is around 6 V, for example Lithium-Ion batteries at 7.2 V with a 750 mAh capacity and mass of 65 g.

The main demand on the batteries is from the DC motors that move the fingers and thumb. Typically, one motor provides a pinch grip to hold a wide range of everyday objects. A standard H-bridge with MOSFETs controls power to the motor. Movement of the fingers and thumb is achievable at full voltage, producing small torques from the motors to overcome losses and any stretching of the elastic glove that covers the prosthesis.

Manoeuvring the fingers and thumb makes only small demands on the batteries. Most of the power is necessary when gripping or squeezing an object. Under this condition, the motors stall and demand maximum current. Heating occurs in the motors and must be limited to preserve the life of the motors.

Typical losses in the MOSFETs are small—approximately 2.5% of the instantaneous battery power is lost for a current of 2 A and a resistance, $R_{DS}(on)$, of 0.05 Ω. The body diodes that return energy from the motor inductance to the supply have a higher voltage drop: 20% of the instantaneous power may be lost when two diodes are forward biased. However, the motor drive dissipates less power if a MOSFET that is in parallel with the body diode conducts during the time that energy returns to the supply. This operation requires a logical co-ordination of the transistor-switching timing. Similarly, freewheeling current can conduct through a diode or, more efficiently, through a MOSFET.

Brushless motors are available specifically for prosthetic use. They provide better mass-to-torque and mass-to-power performance than brushed motors. But, while they reduce mass, they also add to the complexity of electronic operation, requiring rotor-position sensing and additional cables. For example, one three-phase motor requires eight inputs: one power line and one sensor line for each phase with a DC voltage and return zero. Ideally, an electronic circuit would mount close to the motor or integrate at the end of the motor casing so that only two DC supply cables stretch from the actuator to the battery and one signal control line from an electronic controller.

Electronics circuits are required to control the H-bridges. Standard pulse-width-modulation varies the DC voltage a microcontroller applies to the motor terminals.

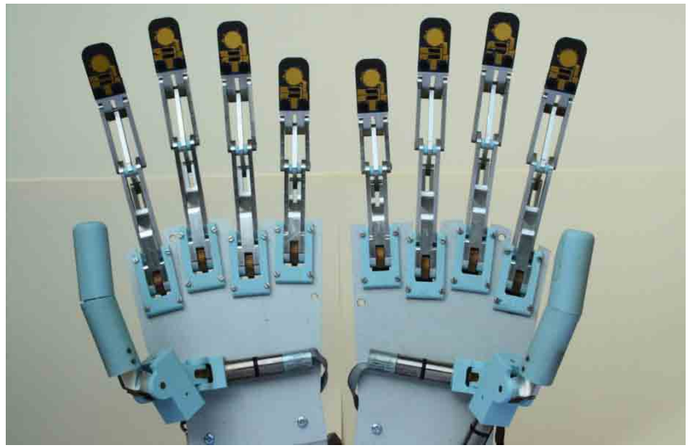

Figure 1: Southampton hands. Across each palm can be seen a dc motor with a worm and wheel to rotate the thumb. Five other motors flex and extend the fingers and thumb. The fingertips have touch (force), slip/texture, and temperature sensors.

Also, electronics are necessary to detect the small voltages from a muscle or two that are used as control inputs from the wearer of the artificial hand. The user inputs are from myoelectric signals that have a random and spiky nature so they are rectified and smoothed to produce analogue or digital signals. Three small electrodes placed on the skin surface above a muscle connect to a low-power instrumentation amplifier that feeds into the microcontroller. The system employs an interface between the controller circuits and H-bridges when the controller operates at a voltage lower than that of the battery (e.g. 3 V). In such cases, a small DC-DC converter steps down the battery voltage.

Historically the development of artificial limbs has progressed during and after international conflicts. Recent events have resulted in further developments of hands with more than one motor to move the fingers individually rather than as a group. With this vision comes a demand for more power from the batteries and additional mass. However rather than relying on only one motor to produce torque, the system can distribute power with additional motors, forming a more efficient grip. The thumb is a dominant feature of any design and so as a compromise, the system could drive the fingers as a group with one motor while operating the thumb with two motors to allow for rotation and, hence, positioning as well as grip. With the need to co-ordinate multiple actuators and to make an artificial hand user-friendly, sensors are added to the design (**Figure 1**). Sensors can free the user from low-level control in much the same way that spinal reflexes and pattern generators automatically co-ordinate natural movement. The sensors measure finger position, force, slip/texture, and temperature. Adding more devices increases power demand so sensors and any subsequent signal processing needs to be minimised. Adding complexity to a prosthetic limb requires more components that consume more power. However, developments in sensors, motor performance, battery technology, and actuation help to lower the mass and increase function.

All the electronics and power management circuits can mount on a single board and occupy a plastic box attached to the plastic socket connecting the artificial hand to the person's residual stump. An industry standard plug and socket (wrist) has electrical connectors to interface the electronics to a hand allowing for easy attachment or detachment of an artificial hand. Circuit boards may be circular and can make use of spaces inside the socket just before the interface or just inside a hand after the plug and socket connection.

The management of power is an area that perhaps has not received the attention that it deserves and with future hand design, there is a need to consider this aspect in the context of the whole system design.

University of Southampton

SPECIAL REPORT : HEALTH, MEDICAL, AND PATIENT MOBILITY

Medical applications demand mixed-signal ICs for high reliability

High-performance low-power signal processing and flexible power management support devices for both clinical and home settings

By: Alison Steer, Product Marketing Manager, Mixed Signal Products, Linear Technology

Advances in medicine and medical treatment bring the promise of more-accurate diagnoses, new treatment methods, and more patient-friendly medical care. From high-resolution imaging systems to drug-delivery systems and implantable electronics, analog, digital, and mixed-signal ICs are playing an expanding role in the medical field. These instruments increasingly require high performance, small size, and low power.

SAR ADCs for medical monitoring

Medical monitoring such as ECG (electrocardiography), EEG (electroencephalography), and pulse oximetry, as well as applications for blood and fluid analysis require precision analog-to-digital conversion with sample rates up to 1 Msps. Depending on the system architecture, 12 to 16-bit SAR-type ADCs are good choices. System requirements for portability in these monitors are driving the need for low-power and small-footprint devices.

For example, Linear Technology's LTC2379-18, 18-bit 250-ksps to 1.6-Msps no-latency SAR ADC family provides a highly competitive SNR performance of 101 dB and -118 dB THD while consuming just 18 mW (**Table 1**). The device automatically powers down between conversions, while linearly reducing the power dissipation as the sampling frequency decreases. The true no-latency operation enables accurate one-shot measurements even after lengthy idle periods with no minimum sample rate required.

Sample Rate	Power Consumption	16-bit 96 dB SNR	18-bit 101 dB SNR
250 ksps	3.75 mW	√	√
500 ksps	7.5 mW	√	√
1 Msps	15 mW	√	√
1.6 Msps	18 mW		√
2 Msps	19 mW	√	

Table 1: The LTC2376 through 2380 pin-compatible family of differential, no-latency SAR ADCs are available in 16- and 18-bit versions.

These devices offer a new digital gain-compression feature that eliminates the need for a negative supply on the ADC driver while preserving the full resolution of the ADC, dramatically lowering the total power consumption of the signal chain. Also included in this pin-compatible family are 250-ksps to 2-Msps 16-bit SAR ADCs with 96.8 dB SNR.

Delta-sigma ADCs for portable monitoring

Medical devices are revolutionizing the home health-care market, allowing monitoring of a variety of health conditions in the home. Technology is enabling portable self-care health systems for observing such vital signs as blood pressure, blood sugar, and temperature.

Home medical-supervision and -monitoring systems allow people to take control of their health, but these medical units must be quick, efficient, and operate reliably. As portable medical sensors evolve, the need

for longer battery life and smaller form factor becomes more critical for noninvasive care.

Some medical measurements require the analog circuitry to run continuously, taking thousands or even millions of readings per second. Other applications require only a single reading per day.

For these occasional tests, the analog circuitry must only power up once, take the measurement, and then sit idle running on a low-power sleep mode the rest of the day. Low-power sleep or nap modes need to be available on the IC to enable low power consumption during the off periods.

For example, Linear offers the LTC2470 family of small, low-cost, 16-bit 1-ksps delta-sigma ADCs with internal references with choice of SPI or I²C interfaces, well suited for portable applications such as patient-wearable ECG monitors with wireless interfaces or temperature and glucose monitors.

High-speed ADCs for medical imaging

Medical imaging applications use a wide range of high-performance data converters. Ultrasound, PET (positron-emission tomography), SPECT (single-photon-emission computed tomography), MRI (magnetic-resonance imaging), and X-ray imaging all use multichannel sampling systems to gather image data. Since these applications require a wide dynamic range, the performance of the ADC is critical.

High SNR and SFDR (spurious-free dynamic range) are necessary for optimal performance. Additionally, in applications such as MRI that use undersampling techniques, wide-bandwidth sample-and-hold performance is critical. Linear Technology has a new line of high-performance, low-power 25- to 125-Msps multichannel ADCs for imaging applications: the dual 16-bit LTC2195, 14-bit and 12-bit quad LTC2175, and dual LTC2268 ADCs with serial LVDS outputs consume a little over 1 mW/Msps per channel.

Power-supply management for medical imaging

Today's high-reliability medical systems require complex digital power management to sequence, supervise, monitor, and margin a large number of voltage rails. It is not unusual for a single application board to have dozens of rails, each with its own unique requirements.

Typically, the power management for these systems requires several discrete devices controlled by an FPGA or a microcontroller around the board to sequence, supervise, monitor, and margin the power supply array. In this scheme, significant time and effort is required to develop the necessary firmware.

Alternatives, such as the LTC2978 octal digital power-supply manager with EEPROM offer medical-system designers integrated, modular power management that reduces debugging time and effort over microcontroller-based designs. The LTC2978 can sequence on, sequence off, monitor, supervise, margin, and trim up to eight power supplies. Multiple LTC2978s can cascade easily using the 1-wire SHARE_CLK bus and one or more bidirectional fault pins.

www.linear.com

Enhancing medical-product usability with IEC 62366

Beyond standards compliance, usability engineering aids competitive differentiation

By: Seppo Vahasalo, Product Line Manager, Medical Devices, SGS

Manufacturers are required by the 3rd edition of IEC 60601-1 to avert the poor usability risks involved in identification, marking, and documents, which can be achieved by an "application of usability engineering to medical devices" compliant with IEC 62366.

Improving usability for safety and competitiveness

The Institute of Medicine issued a report in 1999 entitled *To Err is Human: Building A Safer Health System*. The report contended that over 44,000 people die in US hospitals each year resulting from preventable medical errors, and perhaps as many as 98,000 people. The report stated most medical mistakes are not due to individual carelessness but rather to faulty processes, conditions, and systems that cause people to make errors or fail to avoid making them.

The European MDD and United States FDA both demand that medical devices are developed by taking errors arising from risk-of-use and human factors into account. The IEC 60601-1 3rd edition and specifically IEC 60601-1-6, are examples of international standards that seek to minimize the risks presented by poor usability with the application of usability engineering. There is a responsibility, wherever medical devices are used, to make sure all products on the market are well-designed and ergonomic. The simpler a medical product is to use, the safer it will be for patients. Consequently, safer products increase their market competitiveness.

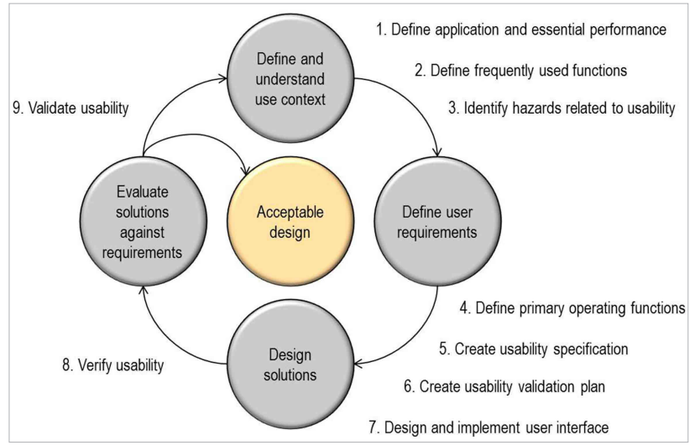

Figure 1: General usability-engineering design cycle

Guidance and implementation of IEC 62366

IEC 62366 provides extensive guidance about how best to minimize the risks with usability engineering. The 100-page document that defines the standard presents a user-interfaced medical design cycle (**figure 1**) within the context of a regulated-product management cycle (**figure 2**).

Table 1 further describes this usability-engineering process and provides an understanding of how IEC 62366 designates design-cycle steps.

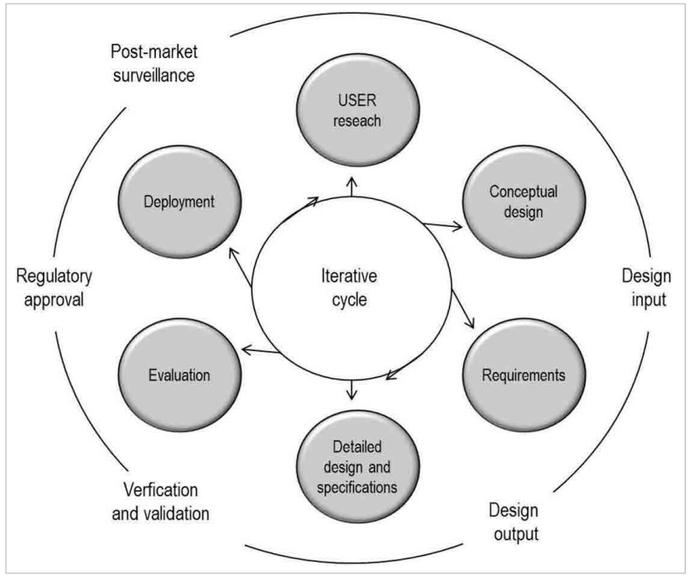

Figure 2: Regulated-product management cycle

Design Cycle Element	IEC 62366 Subclause	Methods
User research/ Conceptual design	5.1 Application specification 5.2 Frequently–used functions 5.3 Identification of characteristics related to safety 5.3.1 Identification of known or foreseeable hazards and hazardous situations	Interviews Observation Questionaires User logbooks Workflow analyses Use cases
Requirement and criteria development	5.4 Primary operating functions 5.5 Usability specification 5.6 Usability validation plan	Functional requirements Usability requirepments: Efficiency Freedom from errors Time to learn
Detailed design and specifications	5.7 User interface design and implementation	Design procedures Style guides
Evaluation	5.8 Usability verfication 5.9 Usability validation 5.3.1 Identification of known or foreseeable hazards and hazardous situations	Expert analysis Heuristic evaluation Cognitive evaluation Reviews User tests: Pair and group tests Observation

Table 1: IEC 62366-compatible usability-engineering process

Updating existing products

Many of the products already in use were not explicitly designed with a usability-engineering process. Proposal 62A/799/DC seeks to address this by initiating an IEC 62366 fast-track amendment to compliance. The proposed amendment introduces an evaluation of UOUP (user-interface of unknown provenance) and a new Annex K to ensure engineering processes include usability in legacy devices, minor revisions of devices, and standard components embedded in medical devices.

Adding good usability to a product is not possible as an afterthought. Design teams should integrate usability engineering from the outset and it is necessary to document the process continuously to comply with IEC 62366. Although the regulations demand usability engineering, good usability can also serve as the basis for product differentiators that offer competitive advantages.

Questioning and observing users to learn how they use various versions of equipment and early prototypes is an invaluable part of the process. When users know how to use a product intuitively and have no need to find workarounds, your product design is certainly going in the right direction. Designing an aesthetically pleasing medical device or software application also reaps dividends.

www.sgs.com/en

As SiC portfolios grow, motor drives beckon

By: David G. Morrison, Editor, How2Power.com

Silicon-carbide technology has the potential to enhance performance in numerous high-power applications. However, many power electronics engineers may have questions about the readiness of SiC power devices for their current design projects and the impact these devices may have on their designs. In a recent article in How2Power Today, Paul Kierstead of Cree assesses the readiness and potential impact SiC MOSFETs and Schottky diodes on motor-drive applications.

In *Silicon Carbide Power Solutions Are Ready To Revolutionize Motor Drives*, Kierstead analyzes the impact of his company's high-performance transistors and diodes on a standard variable-frequency motor drive. The author breaks down the application into its three major power conversion functions:

- the dc-ac power inverter responsible for driving the motor
- the ac-dc rectifier section with built-in regen function and
- the auxiliary power supply that powers digital control and other functions.

Focusing on each of these sections, Kierstead explains how replacing silicon IGBTs and fast-recovery PiN diodes with SiC MOSFETs and Schottkys achieves benefits such as higher efficiency, simplified topologies, reduced parts counts, smaller components, and higher-frequency operation. In particular, data is presented to support the claims of improved efficiency enabled by the SiC devices (**see figure**).

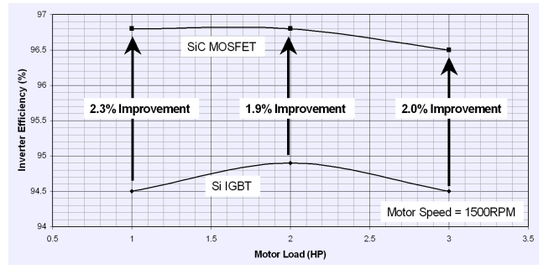

Figure 1a

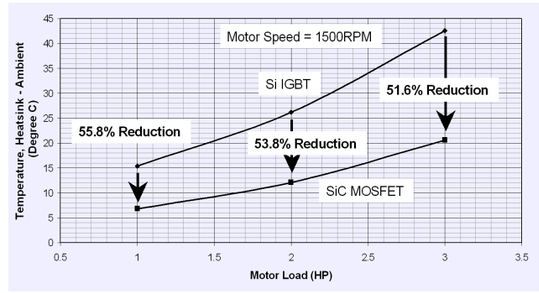

Figure 1b

SiC MOSFETs raise the efficiency of a motor-drive inverter by approximately 2% versus silicon IGBTs (A), while reducing the heatsink temperature (the rise above ambient) by about 50% versus IGBTs (B). (Data courtesy of Cree.)

The author notes that the discussion mainly concerns motor drives operating from mains voltages up to 690 V AC with a 20% high-line value plus design margin. The silicon devices that have been developed for these applications, he says, are pushing the envelope of silicon performance. In contrast, the 1200-V and 1700-V SiC devices now available are barely scratching the surface of SiC's potential. Kierstead observes that SiC devices with 10-kV blocking voltages may be commonplace one day.

The author addresses the reliability issue by pointing to successes achieved with SiC Schottkys (350 billion hours in field operation with

his company's devices), noting their superior failure rate versus silicon diodes. Kierstead predicts that SiC MOSFETs will in time prove to be similarly robust.

This article also touches on the factors that have historically limited SiC's usage in the motor-drive market. These include cost, the lack of device availability with suitable current and voltage ratings, and the lack of power module packaging. The designers' unfamiliarity with the technology has been another factor.

However, as Kierstead explains, today there is a wider array of SiC products (Schottkys, MOSFETs, and JFETs) with device ratings for diodes ranging from 1 to 50 A at blocking voltages from 600 to 1700 V. In addition, SiC power modules in standard and custom configurations are now in development.

To read the full story, see the August 2012 issue of How2Power Today, online at www.how2power.com/newsletters.

About the author:
When not writing this column, David G. Morrison is busy building an exotic power electronics portal called How2Power.com. Do not visit this website if you're looking for the same old, same old. Do come here if you enjoy discovering free technical resources that may help you develop power systems, components, or tools. Also, do not visit How2Power.com if you fancy annoying pop-up ads or having to register to view all the good material. How2Power.com was designed with the engineer's convenience in mind, so it does not offer such features. For a quick musical tour of the website and its monthly newsletter, watch the videos at www.how2power.com and http://www.how2power.com/newsletters/.

www.how2power.com

Flying and national energy awards

By: Gail Purvis, Europe Editor, Power Systems Design

One of the more ominous aspects of flying to "view and see" is the carbon footprint created. Mostly that's just a nasty noise at the back of your head.

Plaudits, thus, to BCD Travel, Germany whose itinerary receipt, painstakingly sets out their traveller's Carbon Footprint Calculator. One person flying to and from Edinburgh to London, for example, racks up 117 kgs or 258 lbs of CO_2 for the 586 miles based on the DEFRA (Department for Environment, Food, and Rural Affairs) calculation model.

The DEFRA model uses emissions factors for short-, medium-, and long-haul flights, of 0.1580, 0.1304, and 0.1056 kgCO_2/km, respectively. These figures derive from more complex emission calculations based on typical fuel burn rates, freight load, seating configuration, and seat class.

Possibly it's what alerted Heineken Breweries to save £250,000 in travel costs and 160 tons of CO_2 in one year using video conferencing—the equivalent of 752 return flights between Edinburgh and London and 2,632 lost hours due to flights.

In another green development, the EBRI (European Bioenergy Research Institute) at Aston University, Birmingham, UK is short-listed for two national energy awards, an Energy Institute Award and the Green Gown Award for its Pyroformer technology.

It seems hard to credit that a machine using a coaxial Archimedes screw system to pyrolyse and chemically process waste material in a single step can really be the ultimate answer to so many of the problems that other renewable energy systems have generated. Yet, EBRI states the Pyroformer has apparently no negative environmental or food security impacts. Its use of multiple feed stocks means it does not require any rainforest destruction or indeed use of agricultural land for bio-crop fuel growth.

The process is emission free and the Pyroformer capable of processing up to 100 kg/h of biomass feed which when coupled with a Gasifier will give it an output sufficient to power 800 homes. The Pyroformer uses a form of intermediate pyrolysis. The reaction temperature for this process is in the range of 450 to 500 °C, with a vapour residence time of a few seconds and a variable residence time for solids. Because the reaction occurs under controlled heating levels it avoids the formation of tar, which is problematic for other forms of pyrolysis due to clogging.

Aston University Professor and EBRI director Andreas Hornung also sees EBRI's work as offering more than just an energy resource. "We believe the Pyroformer will be a key stimulator of growth and jobs and the reaction of the business community so far has been extremely enthusiastic," he says.

November will clearly tell it all.

www.powersystemsdesign.com

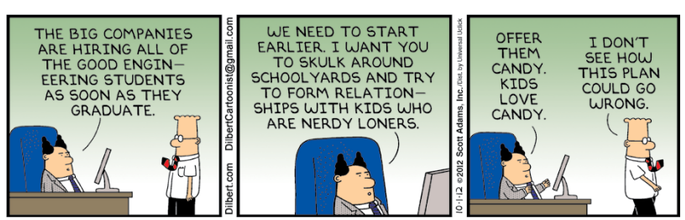

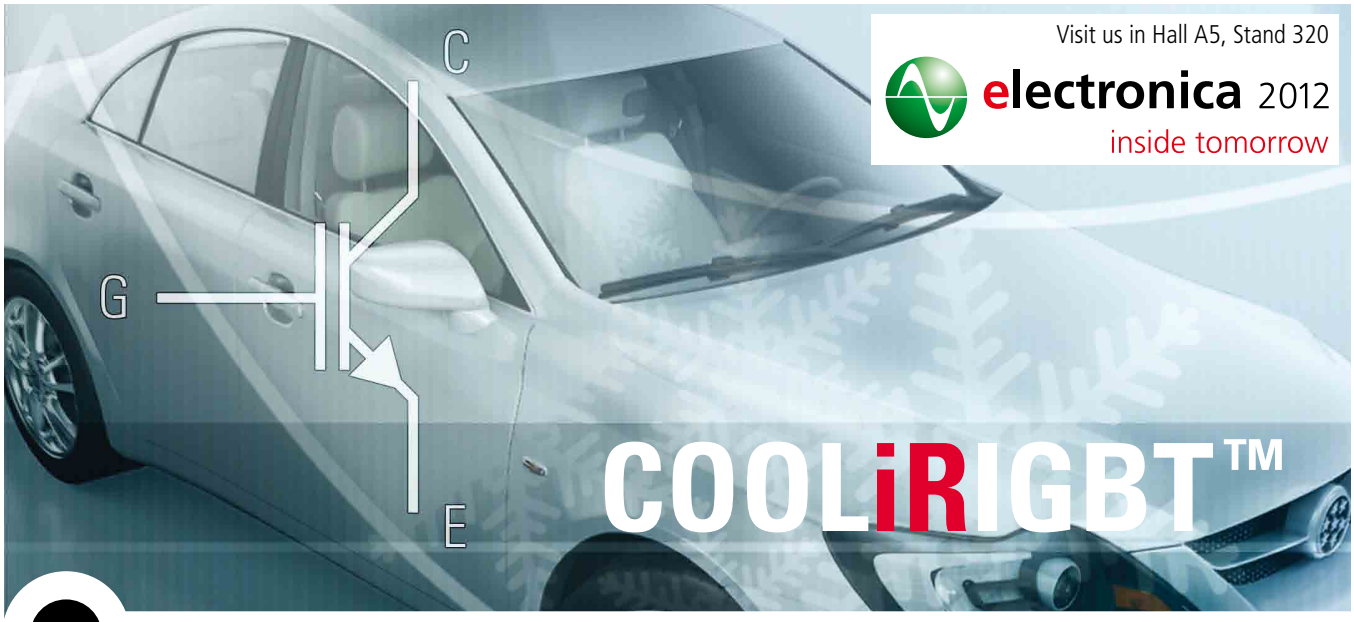

Visit us in Hall A5, Stand 320

electronica 2012

inside tomorrow

Automotive COOLiRIGBT™ Gen 1

Ultra-fast Switching, Rugged 600V High Frequency IGBTs

CooliRIGBT™ offers 50% higher current than super junction MOSFETs

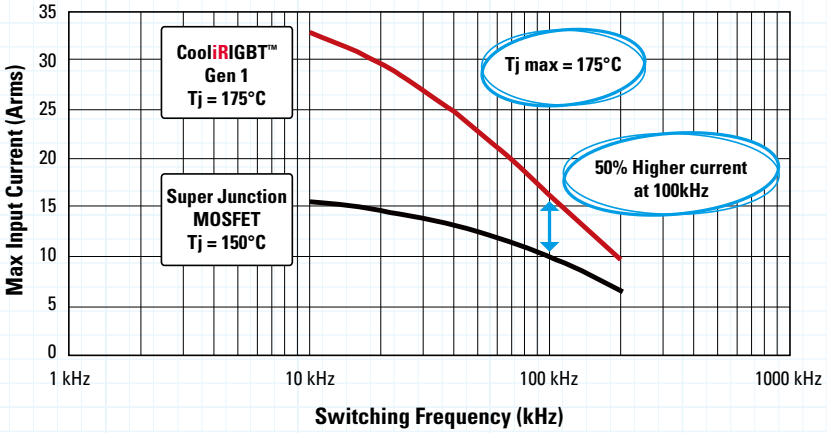

	Super Junction MOSFET	COOLiRIGBT™ Gen1
Tj Max	150°C	175°C
Manufacturability	Complex	Simple
Switching Frequency	High	High
Losses At High Currents	High	Low

COOLiRIGBT™ Gen 1 are designed to be used in a wide range of fast switching applications for electric (EV) and hybrid electric vehicles (HEV) including on-board DC-DC converters, and battery chargers.

Features:

- Switching frequencies up to 200kHz
- 600V rated devices with a short circuit rating of > 5µs
- Low $V_{CE(on)}$
- Positive $V_{CE(on)}$ temperature coefficient making the parts suitable for paralleling
- Square Reverse Bias Safe Operating Area
- Automotive qualified
- Tj max of 175ºC
- Rugged performance
- Designed specifically for automotive applications and manufactured to the 0PPM initiative

For more information call +49 (0) 6102 884 311

or visit us at www.irf.com

International IOR Rectifier

THE POWER MANAGEMENT LEADER